Article

Not peer-reviewed version

A Novel Robust Hybrid Control Strategy for a Quadrotor Trajectory Tracking Aided with Bioinspired Neural Dynamics

Jianqi Li *, Xin Li , Jianquan Lu , Binfang Cao , Jian Sun

Posted Date: 30 August 2024

doi: 10.20944/preprints202408.2173.v1

Keywords: bio-inspired neural dynamics; trajectory tracking; sliding mode control; backstepping control; quadrotor control

 doi:10.20944/preprints202408.2173.v1

Article

A Novel Robust Hybrid Control Strategy for a Quadrotor Trajectory Tracking Aided with Bioinspired Neural Dynamics

Jianqi Li [1,2,3,*], Xin Li [1], Jianquan Lu [3], Binfang Cao [2] and Jian Sun [3]

[1] School of Communication and Electronic Engineering, Jishou University, Jishou, 416000, China; 292596085@qq.com
[2] Hunan Provincial Key Laboratory for Control Technology of Distributed Electric Propulsion Aircraft, Hunan University of Arts and Science, Changde, 415000, China
[3] School of Electrical and Information Engineering, Changsha University of Science and Technology, Changde, 415000, China
* Correspondence: jianqi_li@126.com

Abstract: This paper proposes a novel hybrid control strategy for quadrotor unmanned aerial vehicles (UAVs) based on bio-inspired neural dynamics. This strategy addresses the velocity jump issue prevalent in traditional backstepping control and the control signal chattering problem common in traditional sliding mode control. The control system comprises an outer-loop bio-inspired backstepping controller and an inner-loop bio-inspired sliding mode controller, ensuring smooth trajectory tracking even in the presence of external disturbances. The stability of the quadrotor UAV control system is rigorously analyzed using Lyapunov stability theory. Extensive comparative simulation experiments are conducted to assess the robustness and effectiveness of the control system. Results demonstrate superior trajectory tracking performance of the proposed control system compared to other control systems for quadrotor UAVs.

Keywords: bio-inspired neural dynamics; trajectory tracking; sliding mode control; backstepping control; quadrotor control

1. Introduction

Quadrotor unmanned aerial vehicles (UAVs) are well-suited for various applications, including vertical take-off and landing [1] and flexible trajectory tracking [2]. Consequently, they have garnered significant attention from developers worldwide, stimulating extensive research in this field. Consequently, quadrotor UAVs have found extensive utilization across various civilian domains [3-7]. Nevertheless, the design of a UAV flight control system, be it for autonomous or non-autonomous flight, often presents challenges concerning sensor technology, hardware, and software design. The quadrotor UAV represents a highly complex nonlinear control system that has garnered considerable interest among researchers in the field of automatic control.

Trajectory tracking control has consistently been a focal point of research in the autonomous flight control of quadrotor UAVs. Among the commonly utilized control methods, linear control strategies [8] offer simplicity and ease of design and implementation. However, the inherent nonlinear and strongly coupled characteristics of quadrotor UAV dynamics impose numerous limitations on the effectiveness of these linear control strategies. Moreover, quadrotor UAVs are consistently exposed to external and internal disturbances during autonomous flight operations in complex scenarios, rendering the existing linear control strategies challenging to apply in practical settings.

To address the limitations of linear control strategies, previous studies have proposed various nonlinear control strategies [9-14]. Robust nonlinear control techniques, in general, enhance flight

 doi:10.20944/preprints202408.2173.v1

stability, ensuring satisfactory performance even in the face of unpredictable environmental changes. They enable flexible maneuverability and precise trajectory tracking. Initially, nonlinear control techniques were employed to govern the vertical takeoff and landing (VTOL) of three-degree-of-freedom helicopters [15]. Controller design for quadrotor UAVs poses greater challenges due to the inherent strong coupling between the body frame dynamics and the yaw, pitch, and roll motion, in contrast to helicopters. Numerous studies have explored different nonlinear controllers for diverse autonomous flight control tasks of quadrotor UAVs, including backstepping controllers [10-11], sliding mode controllers [12-13], and other related adaptive nonlinear controllers [14].

The pioneering work of Reference [16] introduced a nonlinear controller for quadrotor aircraft. The authors developed a dynamic feedback controller for hovering flight, utilizing a technique known as exact feedback linearization. The simulation results presented in the paper demonstrated acceptable performance, even in the presence of external disturbances. However, the design of controllers using feedback linearization necessitates an exact model with stable zero dynamics to compensate for the nonlinear terms. However, in practice, the dynamic uncertainty and external disturbances that are inherent in quadrotor flight pose challenges in achieving accurate model predictions, rendering the feedback linearization control strategy infeasible for real-time trajectory tracking control. Consequently, to apply this feedback linearization control strategy in practical applications, it should be augmented with another control strategy that incorporates quadrotor model prediction, as suggested in Reference [17].

The backstepping control strategy [11] is widely employed in robot control as one of the most commonly used methods. Its fundamental principle involves recursively stabilizing a closed-loop backstepping system. Analysis and design of this strategy can be carried out using Lyapunov stability theory. When designing controllers for quadrotor unmanned aerial vehicles using the backstepping control strategy [18], the design of control laws is dependent on the tracking error. Consequently, a significant tracking error leads to a substantial speed jump in the control signal. The power system of the unmanned aerial vehicle cannot immediately realize such an unrealistic speed change. Employing a fuzzy logic control strategy [19] is a practical solution to address the speed jump issue within the aforementioned backstepping control strategy. Nevertheless, the design of fuzzy logic controllers relies on the designer's prior knowledge, posing challenges in formulating satisfactory fuzzy rules tailored to specific environments. Neural network optimization strategy has been employed as a viable solution for addressing similar issues in unmanned aerial vehicles, enabling the computation of complex nonlinear relationships. However, this approach necessitates online learning training, costly computational resources, and a substantial volume of experimental data. Previous studies have explored the implementation of the backstepping control strategy to achieve position tracking control in quadrotor unmanned aerial vehicles; however, the majority of controller designs overlooked the presence of external disturbances.

Previous studies have focused on the development of robust controllers to mitigate the impact of external and internal disturbances on quadrotor unmanned aerial vehicles (UAVs) and ensure stable autonomous flight in challenging environments. One robust control method, the sliding mode control strategy [12], is known for its insensitivity to parameter variance, thereby enhancing the system's resilience to disturbances. However, the control signals generated by the sliding mode control strategy exhibit significant shaking, which can lead to high-frequency variations detrimental to onboard hardware. While attempts have been made to address the shaking problem in existing methods by substituting the shaking term with saturation and tanh functions [20], these solutions compromise robustness to disturbances and necessitate meticulous parameter tuning to mitigate shaking. Furthermore, given the susceptibility of both backstepping control and sliding mode control to noise, control strategies inspired by biological systems can offer smoother control signals, thus effectively resolving the challenges associated with backstepping control and sliding mode control, which is particularly crucial in the context of limited actuators.

Biological neural dynamics, initially proposed by Hodgkin and Huxley [21], refers to the utilization of electrical circuit elements in a patch of membrane within a biological neural system. Yang [22] introduced this bioinspired neural dynamics to the field of robotics, while Zhu [23]

 doi:10.20944/preprints202408.2173.v1

subsequently applied it to the motion control of an underwater unmanned submarine. The overall control design was based on bioinspired neural dynamics and employed a hybrid control approach. A bioinspired backstepping control strategy was employed to address the velocity jump issue in traditional backstepping control, resulting in smooth position control. Additionally, a bioinspired sliding mode control strategy was utilized to tackle the control signal chattering problem in traditional sliding mode control, thereby minimizing the impact on onboard actuators.

The control system for quadrotor unmanned aerial vehicles (UAVs) typically consists of two sub-systems: an outer-loop position control subsystem and an inner-loop attitude control subsystem. In their previous work [11][24], the authors introduced a PID controller for position control and an integral sliding mode controller for attitude control of the quadrotor UAV. Another study [25] presented a terminal sliding mode position controller and a sliding mode attitude controller. Motivated by the characteristics of neural dynamics, this paper presents a robust nonlinear hybrid control strategy based on neural dynamics for quadrotor UAVs. The overall design of the control system includes based on biological neural dynamics backstepping position control subsystem and based on biological neural dynamics sliding mode attitude control subsystem. These subsystems are built upon the dual-loop control structure introduced in [26][27]. The proposed neural dynamics mitigate the speed jump issue commonly encountered in traditional backstepping control methods. Moreover, leveraging the filtering capability of neural dynamics, the control system effectively handles external noise and produces smooth velocity control signals. Furthermore, the integration of neural dynamics with the sliding mode control strategy addresses the control signal chattering problem inherent in traditional sliding mode control, resulting in continuous, smooth, and chattering-free torque control signals.

The paper is organized as follows: Section 2 introduces the kinematic and dynamic models of the quadrotor unmanned aerial vehicle (UAV). In Section 3, a bioinspired neural dynamics model is presented as the foundation for the development of the bioinspired backstepping position controller and the bioinspired sliding mode attitude controller for the quadrotor UAV. The stability analysis of the proposed control system is conducted in Section 3 as well. Section 4 provides the numerical simulation results, which are compared with other control systems to showcase their advantages and effectiveness. Finally, Section 5 summarizes the development philosophy and justifies the superiority of the proposed hybrid control strategy for quadrotor UAVs. The conclusion also includes suggestions for areas of improvement.

2. Dynamical Model

2.1. Quadrotor Model

Using the Newton-Euler equations, the kinematic and dynamic models of the quadrotor unmanned aerial vehicle (UAV) are formulated in two coordinate reference frames: the inertial frame and the body frame [28]. In this study, the inertial frame, denoted as frame $\hat{F}_E = \{\hat{f}_{eo}, \hat{f}_{ex}, \hat{f}_{ey}, \hat{f}_{ez}\}$, while the body frame, denoted as frame $\hat{F}_B = \{\hat{f}_{bo}, \hat{f}_{bx}, \hat{f}_{by}, \hat{f}_{bz}\}$. Here, $\hat{f}_{eo}$ represents the origin of the inertial coordinate system, and $\hat{f}_{bo}$ represents the center of mass of the quadrotor UAV. These definitions are illustrated in Figure 1. The Euler angles of the quadrotor, denoted as $\Theta^E = [\phi \quad \theta \quad \psi]^T \in \mathbb{R}^{3\times1}$, represent its roll angle (ϕ), pitch angle (θ), and yaw angle (ψ). These angles satisfy the conditions $|\phi| < \frac{\pi}{2}$, $|\theta| < \frac{\pi}{2}$, $|\psi| < \pi$. The angular velocities of the drone, denoted as $\Omega^B = [p \quad q \quad r]^T \in \mathbb{R}^{3\times1}$, correspond to its rotations along the X, Y, and Z axes of the body coordinate system, respectively. The position of the quadrotor in the world coordinate system $\hat{F}_E$ is defined as $P^E = [p_x^e \quad p_y^e \quad p_z^e]^T \in \mathbb{R}^{3\times1}$, while the velocity of the quadrotor's movement in the inertial coordinate system $\hat{F}_E$ is defined as $V^E = [v_x^e \quad v_y^e \quad v_z^e]^T \in \mathbb{R}^{3\times1}$. Consequently, the kinematic and dynamic model of the quadrotor's displacement and rotation can be expressed as follows:

$$\dot{P}^E = V^E$$

$$\dot{V}^E = m^{-1}[R_B^E T_B + F_d + dv]$$

Preprints.org (www.preprints.org) | NOT PEER-REVIEWED | Posted: 30 August 2024 doi:10.20944/preprints202408.2173.v1

$$\dot{\Theta}^E = R_\Theta \cdot \Omega^B$$

$$\dot{\Omega}^B = I^{-1}[\tau_b + G_a - \Omega^B \times (I \cdot \Omega^B) + M_d] \quad (1)$$

Where m represents the mass of the quadrotor, I denotes the inertial matrix of the quadrotor in the inertial coordinate system, given by $I = diag(I_{xx},\ I_{yy},\ I_{zz})$, R_B^E signifies the rotation matrix between the body-fixed coordinate system and the inertial coordinate system for the quadrotor's translation, and R_Θ represents the rotation matrix for the quadrotor's rotation. These matrices satisfy the following conditions:

$$R_B^E = \begin{bmatrix} cos\theta cos\psi & sin\phi sin\theta - cos\phi sin\psi & sin\phi sin\psi + cos\phi sin\theta cos\psi \\ cos\theta sin\psi & cos\phi cos\psi + sin\phi sin\theta sin\psi & cos\phi sin\theta sin\psi - cos\psi sin\phi \\ -sin\theta & sin\phi cos\theta & cos\phi cos\theta \end{bmatrix} \quad (2)$$

$$R_\Theta = \begin{bmatrix} 1 & sin\phi tan\theta & cos\phi tan\theta \\ 0 & cos\phi & -sin\phi \\ 0 & sin\phi/cos\theta & cos\phi/cos\theta \end{bmatrix} \quad (3)$$

dv represents step-like increasing values of external disturbances. The variables F_d and M_d represent bounded variations of aerodynamic force and moment, respectively. T_B satisfies $T_B = T_K E_3 - mg(R_B^E)^T E_3$, where g denotes the gravitational constant. T_K represents the total thrust generated by the quadrotor at time t_0, and it can be expressed as $T_K = T_1 + T_2 + T_3 + T_4$. Each $T_i (i = 1,2,3,4)$ represents the thrust $T_i = k_\omega \omega_i^2$ generated by the i-th motor, where k_ω is a positive constant. The variable τ_b describes external torques acting on the x, y, and z axes of the body frame, which satisfy:

$$\tau_b = \begin{bmatrix} l_b b(T_1 - T_2 - T_3 + T_4) \\ l_b b(T_1 + T_2 - T_3 - T_4) \\ k_\tau(T_1 - T_2 + T_3 - T_4) \end{bmatrix} \quad (4)$$

Where, l_b and k_τ represent the body radius and the conversion factor from force to torque, respectively.

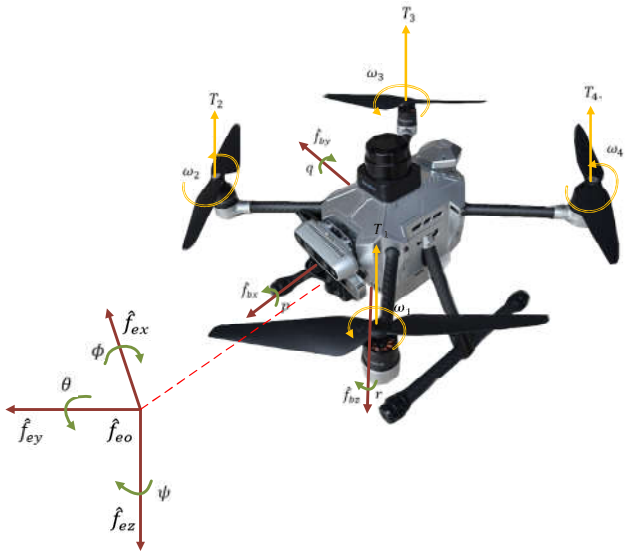

Figure 1. Quadrotor unmanned aerial vehicle (UAV) coordinates in body fixed and inertial frame.

2.2. Control Problem Description

In the above, $P_d^E = [p_{dx}^e \quad p_{dy}^e \quad p_{dz}^e]^T$ and $V_d^E = [v_{dx}^e \quad v_{dy}^e \quad v_{dz}^e]^T$ represent the desired position and velocity of the quadrotor in the inertial frame, respectively. $\Theta_d^E = [\phi_d \quad \theta_d \quad \psi_d]^T$ represents the

 doi:10.20944/preprints202408.2173.v1

desired Euler angles of the quadrotor, and $\Omega_d^B = [\mathrm{p}_d \quad \mathrm{q}_d \quad \mathrm{r}_d]^T$ represents the desired angular velocity of the quadrotor in the body frame. Among these variables, P_d^E and ψ_d serve as inputs to the entire control system. The desired roll angle ϕ_d and pitch angle θ_d are obtained by the outer loop bioinspired backstepping position control system to achieve trajectory tracking. Specifically, the desired position P_d^E and yaw angle ψ_d of the quadrotor are determined based on the tracking trajectory at time t_0. Figure 3 depicts the relationship between tracking errors in the body and inertial coordinate systems during the tracking process. Here, the position error is represented by $e_P = P_d^E - P^E$, the velocity error by $e_V = V_d^E - V^E$, the Euler angle error by $e_\Theta = \Theta_d^E - \Theta^E$, and the body angle error by $e_\Omega = \Omega_d^B - \Omega^B$. The outputs of the relevant controllers are denoted as $u_P = [u_{pi}] \in \mathbb{R}^{3\times1}$, $u_V = [u_{vi}] \in \mathbb{R}^{3\times1}$, $u_\Theta = [u_{\Theta i}] \in \mathbb{R}^{3\times1}$, and $u_\Omega = [u_{\Omega i}] \in \mathbb{R}^{3\times1}$. Specifically, u_P, u_Θ, and $u_{vi}(i = 1,2)$ correspond to the inputs of the velocity controller, angle controller, and angular velocity controller, respectively. They satisfy $V_d^E = u_P$, $\phi_{cd} = u_{v1}$, $\theta_{cd} = u_{v2}$, and $\Omega_d^B = u_\Theta$. u_{v3} and u_Ω represent the control signal inputs for the quadrotor, which drive the four motors to generate total thrust and torque for following the desired trajectory. In this paper, the actual quadrotor dynamical system is treated as a nominal system with the addition of an equivalent disturbance. Therefore, the quadrotor dynamical model can be rewritten as follows:

$$\begin{aligned}
\dot{P}^E &= u_P + \Delta_p \\
\dot{V}^E &= G_V u_V - G + \Delta_v \\
\dot{\Theta}^E &= u_\Theta + \Delta_\Theta \\
\dot{\Omega}^B &= G_\Omega u_\Omega + I^{-1}[G_a - \Omega^B \times (I \cdot \Omega^B)] + \Delta_\Omega
\end{aligned} \tag{5}$$

Where, $G = [0 \quad 0 \quad g]^T$; $G_V = diag(g, -g, k_t/m)$; $G_\Omega = I^{-1}diag(k_{\sigma p}, k_{\sigma q}, k_{\sigma r})$; k_t, $k_{\sigma p}$, $k_{\sigma q}$, and $k_{\sigma r}$ are gain constants of the controller satisfying $T_K = k_t u_{vz}$, $\tau_{bp} = k_{\sigma p} u_{\Omega p}$, $\tau_{bq} = k_{\sigma q} u_{\Omega q}$, and $\tau_{br} = k_{\sigma r} u_{\Omega r}$; $\Delta_i(i = p, v, \Theta, \Omega)$ represents external disturbances and aerodynamics, satisfying:

$$\begin{aligned}
\Delta_p &= V^E - u_P \\
\Delta_v &= \frac{1}{m}(F_d + dv) \\
\Delta_\Theta &= R_\Theta \Omega^B - u_\Theta \\
\Delta_\Omega &= I^{-1} M_d
\end{aligned} \tag{6}$$

3. Quadrotor Control Design Aided with Bioinspired Neural Dynamics

In this section, a hybrid control strategy is developed for a quadcopter drone to address the issues of velocity jumps and control signal chattering in backstepping control and sliding mode control. Figure 3 illustrates the closed-loop control framework, comprising two cascaded control systems. The outer-loop position control system consists of a bioinspired backstepping position controller and velocity controller. The position controller generates smooth velocity commands to prevent abrupt velocity jumps caused by significant tracking errors and external disturbances, while the velocity controller provides desired angular commands. The inner-loop attitude control system utilizes the output angular commands from the outer-loop control system to generate torque control signals for trajectory tracking. To mitigate the control signal chattering problem encountered in traditional sliding mode control, the inner-loop attitude control system incorporates a sliding mode controller with bioinspired neural dynamics.

 doi:10.20944/preprints202408.2173.v1

3.1. Bioinspired Neural Dynamic Model

Hodgkin and Huxley initially proposed a membrane model that utilized electrical elements to describe the behavior of a membrane [26]. Subsequently, Grossberg [30] further advanced this model to capture real-time adaptive behavior in individuals. Yang and Meng [22] were pioneers in applying this model to robots, enabling real-time collision-free motion planning in dynamic environments without the need for prior learning. Over time, this model has been extended to various other robot applications. Referred to as the shunting model, the bioinspired neural dynamics model is expressed as follows:

$$\dot{x}_i = -A_i x_i + (B_i - x_i)S_i^+ - (D_i + x_i)S_i^- \tag{7}$$

In this model, x_i denotes the neural activity of the i-th neuron. A_i represents the passive decay rate, while B_i and D_i represent the upper and lower bounds of the i-th neuron, respectively. The variables S_i^+ and S_i^- indicate the excitatory and inhibitory inputs to the i-th neuron. By utilizing equation (7), the shunting model for the quadcopter can be defined as follows:

$$\dot{E}_i = -A_i E_i + (B_i - E_i)f(e_i) - (E_i - D_i)g(e_i) \tag{8}$$

Where, $e_i(i = P,\ V,\ S)$ represents the inputs to the shunting model, which signifies the error between the desired pose and the quadrotor's state. The functions $f(e_i)$ and $g(e_i)$ are defined as $f(e_i) = \max(e_i, 0)\ and\ g(e_i) = \max(-e_i, 0)$ respectively. E_i denotes the output of the shunting model, and for any input e_i, E_i is constrained within the limits of (B_i, D_i). Given the specific characteristics of the quadcopter drone model, we assume $|B_i| = |D_i|$. Moreover, it is important to highlight that the shunting model exhibits properties similar to those of a low-pass filter, imparting robustness against aerodynamic forces and external disturbances. Subsequent sections will delve into a detailed explanation of the design process for the entire control system.

3.2. Bioinspired Backstepping Position Control System

Designing a backstepping position controller for a quadcopter using Lyapunov functions is relatively straightforward. However, the drone's state and external disturbances can cause unrealistic velocity changes that are not achievable for a drone with limited inputs. To address this issue, this section proposes a bioinspired backstepping position controller that combines the shunting model (Equation 8) with the backstepping control strategy. The focus of this article is primarily on controlling the quadcopter drone to track a spiral ascent trajectory in three-dimensional space, as shown in Figure 2. Therefore, the relationship between the desired position state and the desired velocity state for the drone's trajectory tracking is expressed as:

$$\begin{bmatrix} v_{dx}^e \\ v_{dy}^e \\ v_{dz}^e \end{bmatrix} = \begin{bmatrix} \dot{x}_d \\ \dot{y}_d \\ \dot{z}_d \end{bmatrix} \tag{9}$$

The objective of the outer-loop position control system is to produce control inputs for the thrust, roll angle, and pitch angle. The position controller in the system generates velocity control inputs to drive the quadcopter to a certain speed, thus minimizing the tracking error towards zero. Figure 2 shows the tracking position error in the X, Y, and Z-axis directions of the inertial coordinate system as $e_P = [e_x \quad e_y \quad e_z]^T$, combined with the velocity error obtained from equation (9) as $e_V = [e_{vx} \quad e_{vy} \quad e_{vz}]^T$. Consequently, the position control inputs for the quadcopter, based on the backstepping control approach, are as follows:

$$\begin{aligned} u_V &= G_V^{-1}\left[\ddot{P}_d^E + G + k_V e_V\right] \\ \dot{V}^E &= \ddot{P}_d^E + k_V e_V \\ \dot{P}^E &= V^E = \dot{P}_d^E + k_P e_P \end{aligned} \tag{10}$$

k_P and k_V, respectively. These parameters are defined as $k_P = diag(k_{p1}, k_{p2}, k_{p3})$ and $k_V = diag(k_{v1}, k_{v2}, k_{v3})$. Equation (10) reveals that in scenarios where the drone is in its initial stage or affected by external disturbances, resulting in significant tracking errors in position and velocity, the

Preprints.org (www.preprints.org) | NOT PEER-REVIEWED | Posted: 30 August 2024 doi:10.20944/preprints202408.2173.v1

terms $k_V e_V$ *and* $k_P e_P$ may lead to abrupt changes in velocity during displacement motion. To mitigate this issue, a backstepping control strategy combined with the bioinspired neural dynamics model is proposed. The new virtual control commands are defined as follows:

$$u_V = G_V^{-1}\left[\ddot{P}_d^E + G + k_V E_V\right] \tag{11}$$

Where E_P and E_V represent the outputs of the shunting model for the quadcopter, replacing the position and velocity error inputs, e_P and e_V. The error terms in the virtual control commands must satisfy the following inequality:

$$k_P D_P < k_P E_P < k_P B_P \ , k_V D_V < k_V E_V < +k_V B_V \tag{12}$$

B_P and B_V represent positive constants, while $D_P = -B_P$ and $D_V = -B_V$. Consequently, by carefully selecting appropriate desired velocity $\dot{P}_d^E$ and desired acceleration $\ddot{P}_d^E$, the virtual control command u_V remains within its dynamic constraints and is bounded. Furthermore, thanks to the filtering capability of the bioinspired neural dynamics model, the bioinspired backstepping controller can provide smooth control inputs, even in the presence of noise. The stability of the bioinspired backstepping controller is demonstrated in Section 3.4.

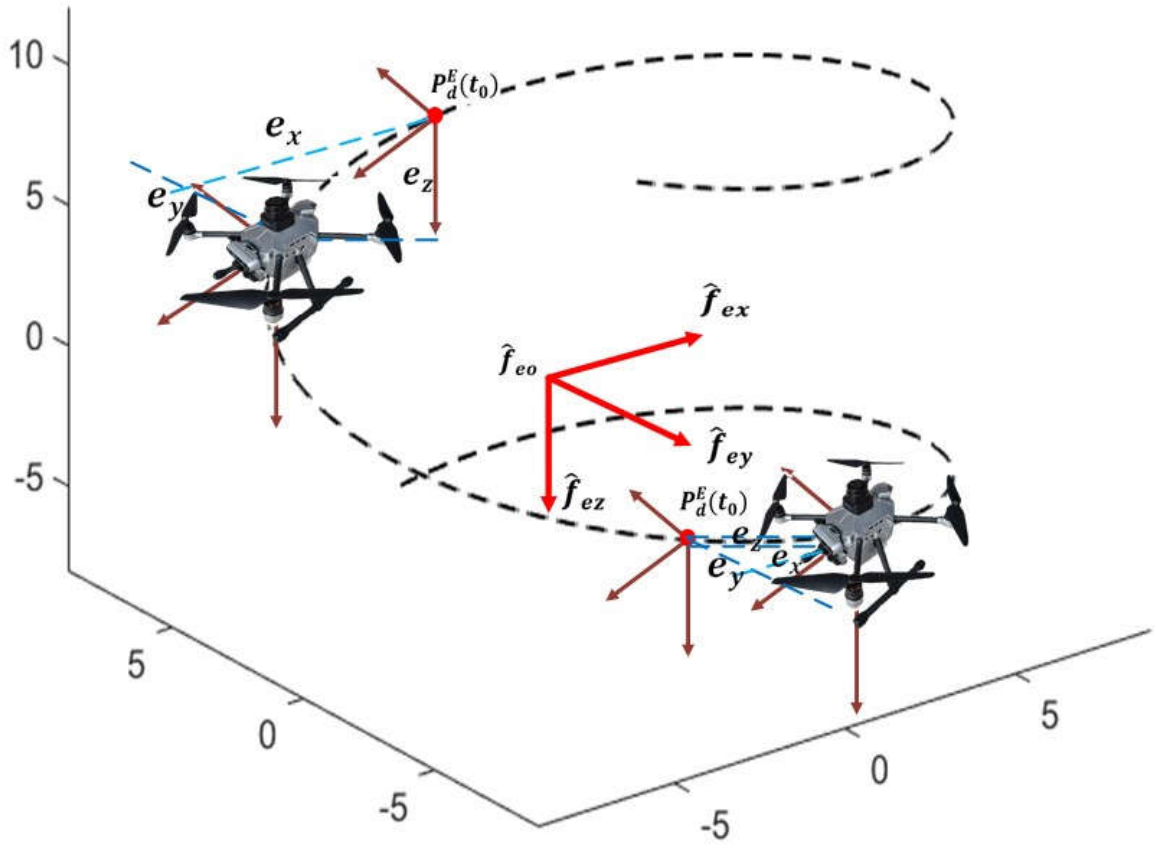

Figure 2. Coordinate conversion for quadrotor unmanned aerial vehicle (UAV).

Preprints.org (www.preprints.org) | NOT PEER-REVIEWED | Posted: 30 August 2024 doi:10.20944/preprints202408.2173.v1

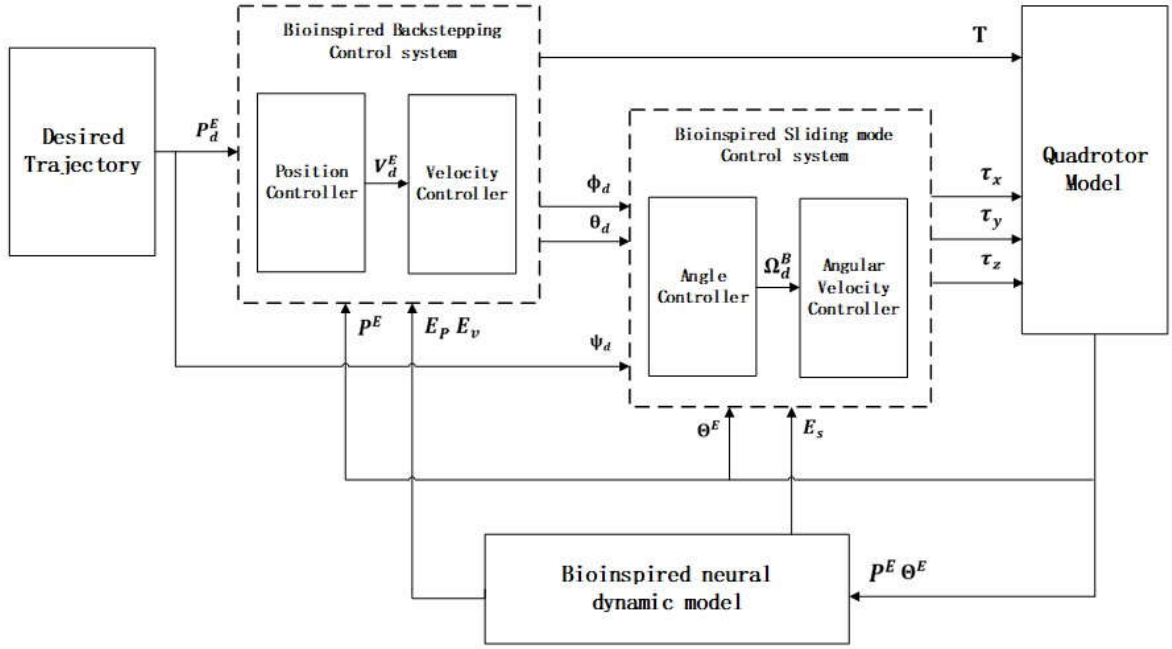

Figure 3. Control system framework for UAV based on the bioinspired hybrid control strategy.

3.3. Bioinspired Sliding Attitude Control System

In this section, we present the development of a robust sliding mode control strategy for a quadcopter drone. The proposed attitude control system combines traditional sliding mode control with the bioinspired neural dynamics model (8) to effectively address the issue of signal chattering commonly encountered in traditional sliding mode controllers. The angle commands u_{v1}, u_{v2} generated by the bioinspired backstepping position control system, along with the desired yaw angle ψ_d, are utilized as inputs to the attitude control system. Subsequently, the bioinspired sliding mode controller generates torque control signals u_Ω to guide the quadcopter drone model towards the desired state.

The defined sliding surface is expressed as follows:

$$S = \dot{e}_\Omega + a_1 e_\Omega + a_2 \int e_\Omega \tag{13}$$

Where a_1 and a_2 are defined as positive constants. Taking the derivative of equation (13), we have:

$$\dot{S} = \ddot{e}_\Omega + a_1 \dot{e}_\Omega + a_2 e_\Omega \tag{14}$$

From equation (14), we can see that when the system operates on the sliding surface $\dot{S} = 0$, we have:

$$\ddot{e}_\Omega + a_1\left(\dot{\Omega}_d^B - \dot{\Omega}^B\right) + a_2 e_\Omega = 0 \tag{15}$$

By substituting the quadcopter dynamics model (5) into equation (15), we obtain:

$$\ddot{e}_\Omega + a_1\left(\dot{\Omega}_d^B - (G_\Omega u_\Omega + I^{-1}[G_a - \Omega^B \times (I \cdot \Omega^B)] + \Delta_\Omega)\right) + a_2 e_\Omega = 0 \tag{16}$$

Therefore, the design of the equivalent control law is given by:

$$u_q = G_\Omega^{-1}\left(\frac{1}{a_1}(\ddot{e}_\Omega + a_2 e_\Omega) + \dot{\Omega}_d^B - I^{-1}[G_a - \Omega^B \times (I \cdot \Omega^B)] - D_\Omega\right) \tag{17}$$

Where D_Ω represents the compensation for aerodynamic moments by the sliding mode controller, satisfying:

$$D_\Omega = d_{\Omega 2} - d_{\Omega 1} sgn(S) \tag{18}$$

$d_{\Omega 1} = (\delta_U + \delta_L)/2$ and $d_{\Omega 2} = (\delta_L - \delta_U)/2$, where δ_U represents the upper bound of the aerodynamic moment and δ_L represents the lower bound. Due to the computational challenges in

 doi:10.20944/preprints202408.2173.v1

calculating $\ddot{e}_\Omega$ as stated in equation (17), an approximation can be made by defining $\ddot{e}_\Omega = k_e \dot{e}_\Omega$, where k_e represents a feedback control gain. The conventional sliding mode control law can be expressed as follows:

$$u_\Omega = u_q + k_s sgn(S) \tag{19}$$

Chattering in traditional sliding mode control signals is a result of the sign function sgn(·). To mitigate this issue, a commonly used approach is to substitute the sign function with a saturation function. Consequently, the sliding mode control law incorporating the saturation function can be expressed as follows:

$$u_\Omega = u_q + k_s sat(S)$$

$$sat(S) = \begin{cases} B_S \ , & k_s S > B_S \\ k_s S \ , & B_S \geq k_s S \geq B_S \\ D_S \ , & D_S > k_s S \end{cases} \tag{20}$$

Where B_S and D_S denote the upper and lower bounds of the saturation function, respectively. Although the saturation function effectively reduces control signal chattering in the presence of small control signals, it may not be suitable for all applications in complex operating environments where larger control signals are necessary to ensure stable flight. To address this limitation, a combination of biologically inspired neural dynamics (equation 8) and sliding mode control is proposed. The resulting biologically inspired sliding mode control commands are defined as follows:

$$u_\Omega = u_q + E_S \tag{21}$$

The proposed biologically inspired sliding mode controller in this paper effectively mitigates the problem of control signal chattering that is commonly encountered in traditional sliding mode control methods. Moreover, it demonstrates excellent trajectory tracking performance even in complex scenarios.

3.4. Stability Analysis

This paper presents a novel approach to achieve progressive trajectory tracking control by integrating a bioinspired neural network control strategy with the aerodynamics and external disturbances of a quadrotor unmanned aerial vehicle. The asymptotic stability of both control systems is verified through rigorous Lyapunov stability analysis. Additionally, by constructing a global Lyapunov candidate function, the study establishes the global asymptotic stability of the proposed control system.

To demonstrate the stability of the bioinspired backstepping controller, the Lyapunov function is defined as follows:

$$V_P = \frac{1}{2} e_P^2 + \frac{1}{2} e_V^2 + \frac{k_P}{2B_P} E_P^2 + \frac{k_V}{2B_V} E_V^2 \tag{22}$$

Then, the derivative of V_P is denoted as:

$$\dot{V}_P = e_P \dot{e}_P + e_V \dot{e}_V + \frac{k_P}{B_P} E_P \dot{E}_P + \frac{k_V}{B_V} E_V \dot{E}_V \tag{23}$$

Splitting the time derivative expression (23) of the candidate function into two components, we have: $e_P \dot{e}_P + e_V \dot{e}_V$ and $\frac{k_P}{B_P} E_P \dot{E}_P + \frac{k_V}{B_V} E_V \dot{E}_V$. Based on the tracking errors and equation (10), $e_P \dot{e}_P + e_V \dot{e}_V$ can be written as:

$$\begin{aligned} e_P \dot{e}_P + e_V \dot{e}_V &= e_P \left(\dot{P}_d^E - \dot{P}^E \right) + e_V \left(\dot{V}_d^E - \dot{V}^E \right) \\ &= -k_P E_P e_P - k_V E_V e_V \end{aligned} \tag{24}$$

 doi:10.20944/preprints202408.2173.v1

For the second part, , $\frac{k_P}{B_P}E_P\dot{E}_P + \frac{k_V}{B_V}E_V\dot{E}_V$, of the Lyapunov function, considering the specific characteristics of the quadrotor unmanned aerial vehicle model, let's assume $B_P = -D_P$ and $B_V = -D_V$. Based on the biological neural dynamics model equation (8), the second part can be written as:

$$\begin{aligned}
&\frac{k_P}{B_P}E_P\dot{E}_P + \frac{k_V}{B_V}E_V\dot{E}_V \\
&\quad = \frac{k_P}{B_P}E_P\big(-A_PE_P + (B_P - E_P)f(e_P) \\
&\quad - (E_P - D_P)g(e_P)\big) \\
&+ \frac{k_V}{B_V}E_V(-A_VE_V + (B_V - E_V)f(e_V) - (E_V - D_V)g(e_V)) \\
&= \frac{k_P}{B_P}E_P^2\big(-A_P - f(e_P) - g(e_P)\big) + k_PE_P\big(f(e_P) - g(e_P)\big) \\
&+ \frac{k_V}{B_V}E_V^2\big(-A_V - f(e_V) - g(e_V)\big) + k_VE_V\big(f(e_V) - g(e_V)\big) \qquad (25)
\end{aligned}$$

Combining equations (24) and (25), we can infer that:

$$\begin{aligned}
\dot{V}_P = &\frac{k_P}{B_P}E_P\big(-A_PE_P + (B_P - E_P)f(e_P) - (E_P - D_P)g(e_P)\big) \\
&+ \frac{k_V}{B_V}E_V(-A_VE_V + (B_V - E_V)f(e_V) - (E_V - D_V)g(e_V)) \\
= &\frac{k_P}{B_P}E_P^2\big(-A_P - f(e_P) - g(e_P)\big) + k_PE_P(f(e_P) - g(e_P) - e_P) \\
&+ \frac{k_V}{B_V}E_V^2\big(-A_V - f(e_V) - g(e_V)\big) + k_VE_V(f(e_V) - g(e_V) - e_V) \qquad (26)
\end{aligned}$$

According to the equation (8), we can conclude that:

$$\begin{cases} f(e_i) = e_i \quad g(e_i) = 0 & , \ e_i \geq 0 \\ f(e_i) = 0 \quad g(e_i) = -e_i & , \ e_i < 0 \end{cases} \qquad (27)$$

By using formula (27), we obtain:

$$\begin{aligned}
-A_i - f(e_i) - g(e_i) < 0 \\
f(e_i) - \ g(e_i) = e_i \qquad (28)
\end{aligned}$$

From equations (22), (26), and (28), it can be inferred that as $t \to \infty$, $V_P \to 0$ and $\dot{V}_P$ is negative definite. V_P can only be zero when $e_i = \mathbf{0}^{3\times1}$. Therefore, the bioinspired backstepping position control system designed in this paper is asymptotically stable.

To prove the stability of the bioinspired sliding mode controller, the designed Lyapunov function is defined as follows:

$$V_\Theta = -\frac{1}{2}S^TS + \frac{1}{2\,B_S}E_S^TE_S \qquad (29)$$

Differentiating the Lyapunov equation, we obtain:

$$\dot{V}_\Theta = -S^T\dot{S} + \frac{1}{B_S}\dot{E}_S^TE_S \qquad (30)$$

Combining the biological neural dynamics model (8) with equation (30), we have:

$$\dot{V}_\Theta = -S^T(\ddot{e}_\Omega + a_1\dot{e}_\Omega + a_2e_\Omega)$$

 doi:10.20944/preprints202408.2173.v1

$$+\frac{1}{B_S}E_S\left(-A_S{}^T E_S{}^T+\left(B_S{}^T-E_S{}^T\right)f^T(S)-\left(E_S{}^T-D_S{}^T\right)g^T(S)\right)$$

$$=-S^T(\ddot{e}_\Omega+a_1\dot{e}_\Omega+a_2e_\Omega)+\frac{1}{B_S}E_SE_S{}^T\left(-A_S{}^T-f^T(S)-g^T(S)\right)$$

$$+\frac{1}{B_S}E_S\left(B_S{}^Tf^T(S)+D_S{}^Tg^T(S)\right) \quad (31)$$

Combining formulas (5), formula (31) can be written as:

$$\dot{V}_\Theta=-S^TE_S+\frac{1}{B_S}E_SE_S{}^T\left(-A_S{}^T-f^T(S)-g^T(S)\right)$$

$$+\frac{1}{B_S}E_S\left(B_S{}^Tf^T(S)+D_S{}^Tg^T(S)\right) \quad (32)$$

Where, $B_S{}^T=-D_S{}^T$ *and* $B_S{}^T=B_S$, rewriting equation (32), we have:

$$\dot{V}_\Theta=\frac{1}{B_S}E_SE_S{}^T\left(-A_S{}^T-f^T(S)-g^T(S)\right)+E_S(f^T(S)-g^T(S)-S^T) \quad (33)$$

Based on formulas (27) and (28), we can also observe that $\frac{1}{B_S}E_SE_S{}^T\left(-A_S{}^T-f^T(S)-g^T(S)\right)<0$ *and* $E_S(f^T(S)-g^T(S)-S^T)=0$. From the biological neural dynamics model (8), as $t\to\infty$, $S\to 0$, and E_S also tends to 0. It follows that $V_\Theta\to 0$, $\dot{V}_\Theta$ is negative definite, and V_Θ can only be zero when $S=0$. Therefore, the designed bioinspired sliding mode attitude control system is asymptotically stable.

To demonstrate the stability of the entire control system, the Lyapunov function of the system and its time derivative are designed as follows:

$$V=V_P+V_\Theta$$

$$\dot{V}=\dot{V}_P+\dot{V}_\Theta \quad (34)$$

The results obtained from equations (26) and (33) can prove that the entire control system is asymptotically stable.

4. Results

In this study, we validate the efficacy of the proposed hybrid control strategy through comprehensive numerical simulations conducted using MATLAB/Simulink. We employ the quadrotor unmanned aerial vehicle model described in equation (1), and the specific model parameters are documented in Table 1. To evaluate the robustness and effectiveness of our control approach, we examine two scenarios: an ideal environment devoid of disturbances and a more intricate application setting featuring step-wise ascending disturbances. The simulations are conducted over a duration of 100 seconds.

Table 1. Quadrotor model Parameters.

Symbol	Value
m	0.18 kg
g	9.81 m/s^2
l_b	0.225 m
b	2.9×10^{-6} Ns^2/rad^2
k_τ	1.779×10^{-7} Ns^2/rad^2
I_{xx}	2.5×10^{-4} m/s^2
I_{yy}	2.5×10^{-4} m/s^2
I_{zz}	3.738×10^{-4} m/s^2

Preprints.org (www.preprints.org) | NOT PEER-REVIEWED | Posted: 30 August 2024 doi:10.20944/preprints202408.2173.v1

4.1. Undisturbed Trajectory Tracking

To assess the trajectory tracking capabilities of our proposed hybrid control strategy, we assume a continuous and differentiable desired tracking trajectory. The chosen trajectory is defined as $x_d = 8sin(0.1t)$, $y_d = 8sin\left(0.1t + \frac{1}{2}\pi\right)$, $z_d = -8 + 0.2t$, with a constant desired yaw angle ψ_d of zero. Initially, the body is positioned at $P^E = [0 \quad 0 \quad -8]^T$, while the velocities $V^E = \Theta^E = \Omega^B = \mathbf{0^{3\times 1}}$. We conduct numerical simulations in the absence of disturbances, utilizing the control parameters listed in Table 2. Figure 4 illustrates the performance of our proposed control method, which exhibits slight deviations compared to other control methods [31-33].

Table 2. Controller Parameters.

Symbol	Value
k_t	0.6
G_Ω	$I^{-1}diag(1,1,1)$
A_P	$diag(-0.4,-0.4,-0.4)$
B_P	$diag(0.8\,,0.8\,,0.8)$
D_P	$diag(-0.8\,,-0.8\,,-0.8)$
A_V	$diag(-0.25,-0.25,-0.25)$
B_V	$diag(1\,,1\,,1)$
D_V	$diag(-1\,,-1\,,-1)$
A_S	$diag(-0.825,-0.825,-0.825)$
B_S	$diag(1.8\,,1.8\,,1.8)$
D_S	$diag(-1.8\,,-1.8\,,-1.8)$
K_P	$diag(1.48\,,1.48\,,1.2)$
K_V	$diag(6\,,6\,,4.8)$
a_1	$diag(0.1\,,0.1\,,0.1)$
a_2	$diag(0.01\,,0.01\,,0.01)$

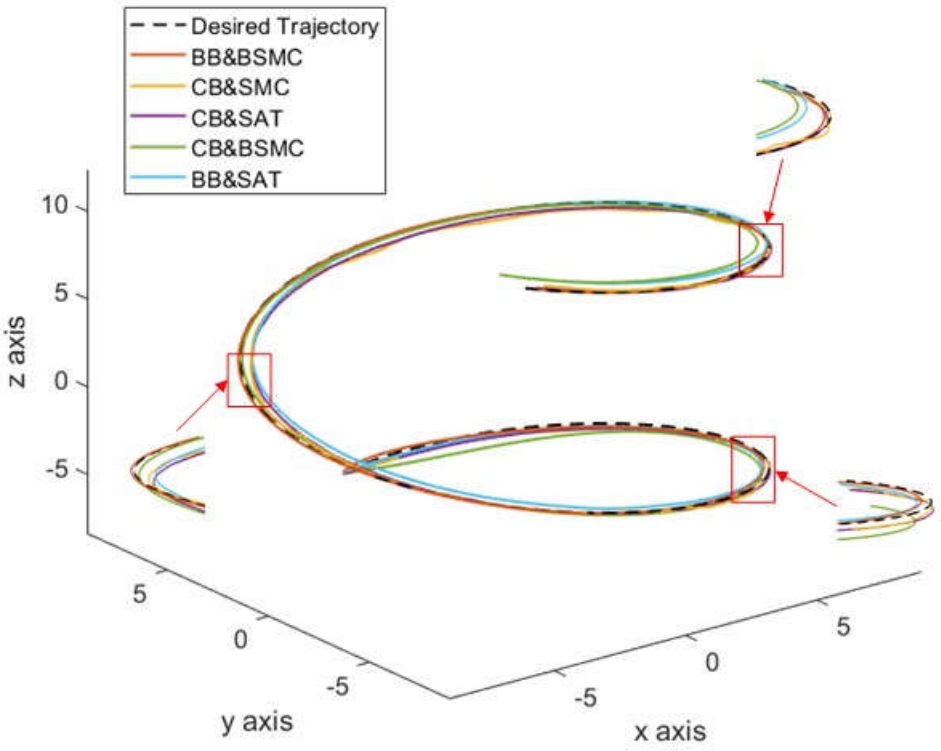

Figure 4. Trajectory tracking performance. CB, Traditional Backstepping [12]; SMC, Traditional Sliding mode [32] SAT, Sliding mode with saturation [19]; BB, Bioinspired Backstepping; BSMC, Bioinspired Sliding mode.

 doi:10.20944/preprints202408.2173.v1

In comparison to other control methods, the proposed approach demonstrates superior trajectory tracking performance. While the traditional backstepping control strategy results in a shorter time for the unmanned aerial vehicle to reach the desired trajectory compared to the bioinspired backstepping control strategy, Figure 5 shows that the velocity commands generated by the former exhibit abrupt changes. On the other hand, the bioinspired hybrid control method produces smoother velocity commands without any jumps. The abrupt change in velocity commands is a crucial issue for practical applications of unmanned aerial vehicles because it demands the immediate attainment of unrealistic velocities and torques when there is a significant initial error, which is not achievable with existing actuators. Furthermore, this issue may pose a risk of crashes during flight. Therefore, the bioinspired backstepping control strategy effectively addresses this problem.

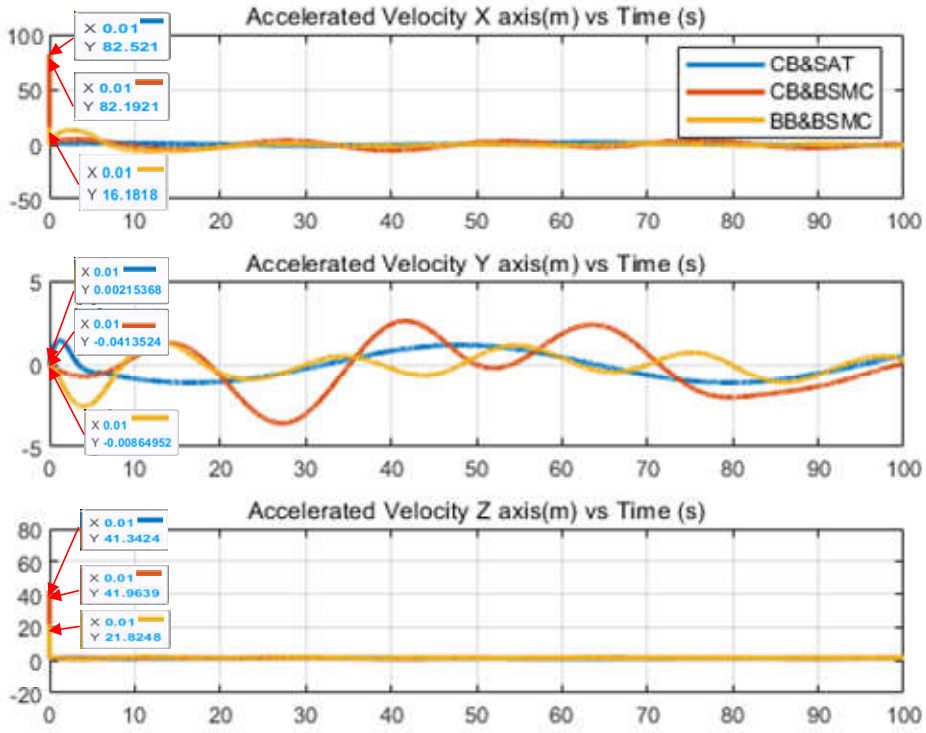

Figure 5. Acceleration Commands. Blue, Traditional Backstepping and Sliding mode with saturation; Red, Traditional Backstepping and Bioinspired Sliding mode; Yellow, Bioinspired Backstepping and Bioinspired Sliding mode.

Furthermore, from Figure 6a, it can be observed that the traditional sliding mode control strategy suffers from control signal chattering, which imposes a significant burden on the onboard actuators. In contrast, the proposed bio-inspired sliding mode controller effectively avoids this issue and provides smooth torque control inputs. The combination of saturation function and sliding mode control is a common approach that can effectively mitigate the chattering problem associated with some traditional sliding mode control methods. However, when the tracking error e_Ω is outside the interval defined by B_Ω and D_Ω, the control signal may still exhibit chattering. When the unmanned aerial vehicle operates in a complex environment, it is challenging to tune the control parameters of the saturation function to achieve satisfactory performance under varying flight conditions. As shown in Figure 6b, although the chattering problem is partially addressed, some chattering still persists. Hence, the saturation function alone cannot fully resolve the chattering issue in traditional sliding mode control, while the bio-inspired sliding mode control strategy, as observed from Figure 6, demonstrates good performance in handling chattering.

Preprints.org (www.preprints.org) | NOT PEER-REVIEWED | Posted: 30 August 2024 doi:10.20944/preprints202408.2173.v1

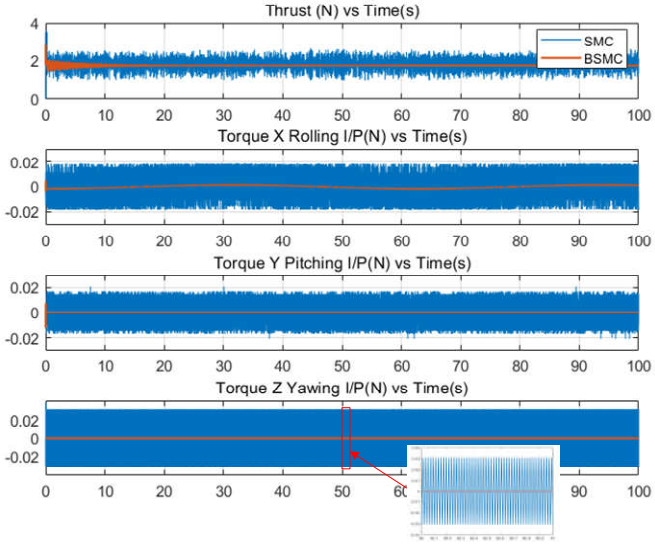

(a) Blue, Traditional Sliding mode; Red, Bioinspired Sliding mode

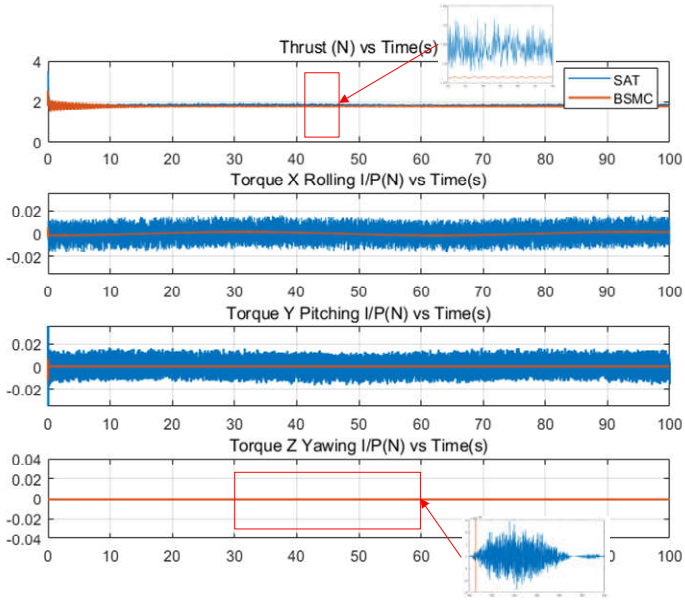

(b) Blue, Sliding mode with saturation; Red, Bioinspired Sliding mode

Figure 6. Thrust and Torque Commands.

4.2. Disturbed Trajectory Tracking

In this section, we investigate an application scenario characterized by step-wise ascending external disturbances as shown in Figure 7, which are caused by adverse weather conditions such as gusts directly impacting the aircraft's center of mass. This scenario aims to assess the robustness of the proposed hybrid control strategy. The control parameters remain consistent with those presented in Table 2, demonstrating reduced reliance on parameters compared to conventional backstepping and sliding mode control approaches. From Figures 8–10, it is evident that the proposed control strategy exhibits smoother tracking trajectories and velocity changes in the presence of external disturbances, while maintaining consistent tracking performance thereafter.

Preprints.org (www.preprints.org) | NOT PEER-REVIEWED | Posted: 30 August 2024 doi:10.20944/preprints202408.2173.v1

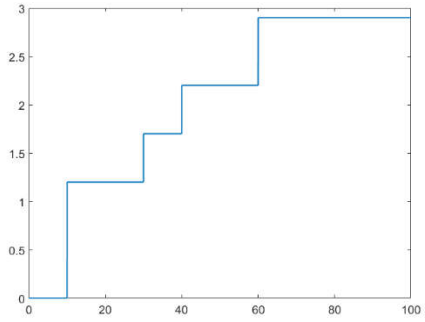

Figure 7. Step-wise ascending Disturbance signal.

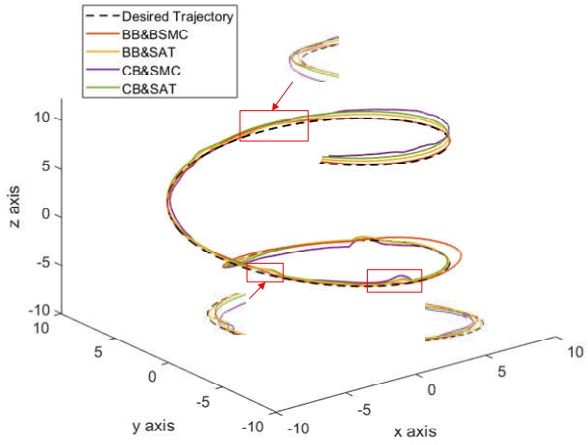

Figure 8. Trajectory tracking performance with disturbance. CB, Traditional Backstepping [35]; SMC, Traditional Sliding mode [35] SAT, Sliding mode with saturation [19]; BB, Bioinspired Backstepping; BSMC, Bioinspired Sliding mode.

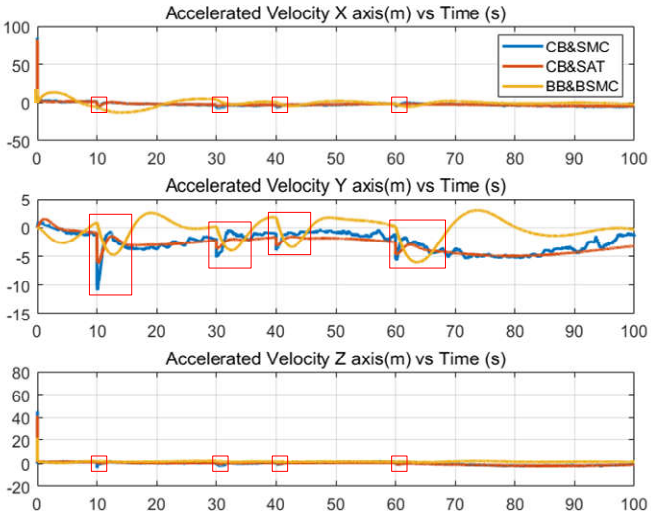

Figure 9. Acceleration Commands with disturbance. Blue, Traditional Backstepping and Sliding mode with saturation; Red, Traditional Backstepping and Bioinspired Sliding mode; Yellow, Bioinspired Backstepping and Bioinspired Sliding mode.

 doi:10.20944/preprints202408.2173.v1

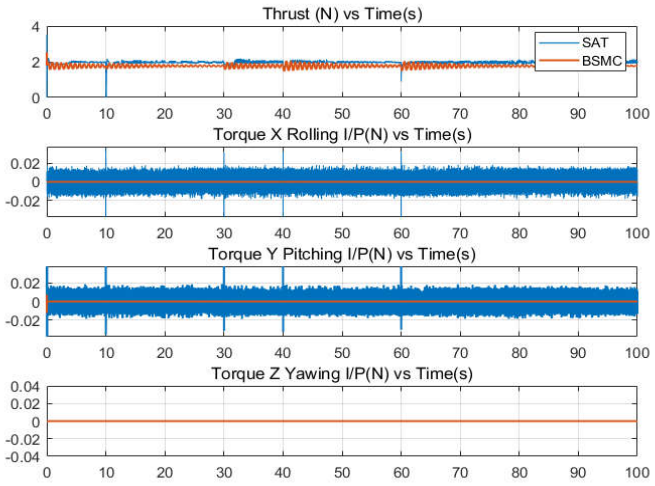

(a) Blue, Traditional Sliding mode; Red, Bioinspired Sliding mode

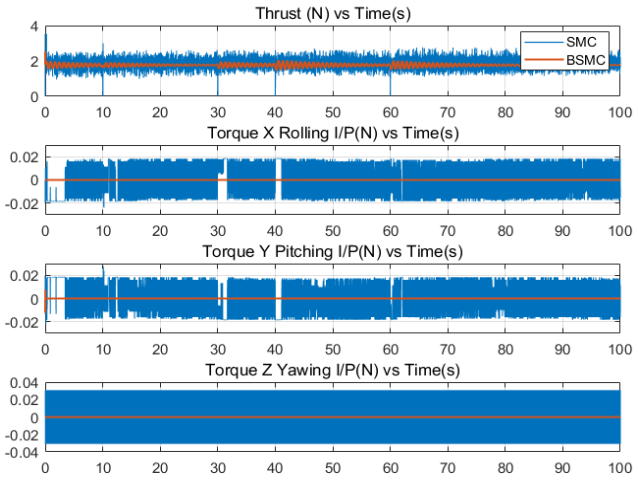

(b) Blue, Sliding mode with saturation; Red, Bioinspired Sliding mode

Figure 10. Thrust and Torque Commands with disturbance.

5. Conclusions

This paper introduces a novel hybrid control strategy for quadrotor unmanned aerial vehicles (UAVs) based on bioinspired neural dynamics. The control system comprises an outer-loop bioinspired backstepping controller and an inner-loop bioinspired sliding mode controller, addressing the challenges of velocity jumps in traditional backstepping control and control signal chattering in traditional sliding mode control. Furthermore, the proposed control system ensures smooth tracking trajectories even in the presence of external disturbances. The stability of the quadrotor UAV control system is rigorously analyzed using Lyapunov stability theory. Extensive comparative simulation experiments are conducted to assess the robustness and effectiveness of the control system. The results unequivocally demonstrate superior trajectory tracking performance of the proposed control system compared to other control systems for quadrotor UAVs. Future research should include the incorporation of precise state estimation techniques to account for the impact of actuator delays on trajectory tracking.

 doi:10.20944/preprints202408.2173.v1

Funding: This work was supported by the National Natural Science Foundation of China (No. 62273142), the Hunan Province Natural Science Foundation, China (No. 2023JJ30437) and the science and technology innovation Program of Hunan Province (No. 2021GK2010).

References

1. B. Erginer and E. Altug, "Modeling and PD Control of a Quadrotor VTOL Vehicle," 2007 IEEE Intelligent Vehicles Symposium, Istanbul, Turkey, 2007, pp. 894-899, doi: 10.1109/IVS.2007.4290230.
2. Y. Wu, J. Sun and Y. Yu, "Trajectory tracking control of a quadrotor UAV under external disturbances based on linear ADRC," 2016 31st Youth Academic Annual Conference of Chinese Association of Automation (YAC), Wuhan, China, 2016, pp. 13-18, doi: 10.1109/YAC.2016.7804858.
3. Grzonka, Slawomir, Giorgio Grisetti, and Wolfram Burgard. "A fully autonomous indoor quadrotor." IEEE Transactions on Robotics 28.1 (2011): 90-100.
4. Ghadiok, Vaibhav, Jeremy Goldin, and Wei Ren. "On the design and development of attitude stabilization, vision-based navigation, and aerial gripping for a low-cost quadrotor." Autonomous Robots 33.1-2 (2012): 41-68.
5. Mohd Basri, Mohd Ariffanan, Abdul Rashid Husain, and Kumeresan A. Danapalasingam. "Enhanced backstepping controller design with application to autonomous quadrotor unmanned aerial vehicle." Journal of Intelligent & Robotic Systems 79 (2015): 295-321.
6. Shauqee, Mohamad Norherman, Parvathy Rajendran, and Nurulasikin Mohd Suhadis. "An effective proportional-double derivative-linear quadratic regulator controller for quadcopter attitude and altitude control." Automatika: časopis za automatiku, mjerenje, elektroniku, računarstvo i komunikacije 62.3-4 (2021): 415-433.
7. Dydek, Zachary T., Anuradha M. Annaswamy, and Eugene Lavretsky. "Adaptive control of quadrotor UAVs: A design trade study with flight evaluations." IEEE Transactions on control systems technology 21.4 (2012): 1400-1406.
8. Koivo, A., and Ten-Huei Guo. "Adaptive linear controller for robotic manipulators." IEEE Transactions on Automatic Control 28.2 (1983): 162-171.
9. Mokhtari, Abdellah, Abdelaziz Benallegue, and Boubaker Daachi. "Robust feedback linearization and GH/sub/spl infin//controller for a quadrotor unmanned aerial vehicle." 2005 IEEE/RSJ International Conference on Intelligent Robots and Systems. IEEE, 2005.
10. Chen, Fuyang, et al. "A novel nonlinear resilient control for a quadrotor UAV via backstepping control and nonlinear disturbance observer." Nonlinear Dynamics 85 (2016): 1281-1295.
11. Thanh, Ha Le Nhu Ngoc, et al. "Quadcopter UAVs Extended States/Disturbance Observer-Based Nonlinear Robust Backstepping Control." Sensors 22.14 (2022): 5082.
12. Weidong, Zhou, et al. "Position and attitude tracking control for a quadrotor UAV based on terminal sliding mode control." 2015 34th Chinese control conference (CCC). IEEE, 2015.
13. Noordin, Aminurrashid, et al. "Adaptive PID controller using sliding mode control approaches for quadrotor UAV attitude and position stabilization." Arabian Journal for Science and Engineering 46 (2021): 963-981.
14. Mohammadi, Mostafa, and Alireza Mohammad Shahri. "Adaptive nonlinear stabilization control for a quadrotor UAV: Theory, simulation and experimentation." Journal of Intelligent & Robotic Systems 72 (2013): 105-122.
15. Isidori, Alberto, et al. "Robust nonlinear motion control of a helicopter." Robust Autonomous Guidance: An Internal Model Approach (2003): 149-192.
16. Mistler, V., Abdelaziz Benallegue, and N. K. M'sirdi. "Exact linearization and noninteracting control of a 4 rotors helicopter via dynamic feedback." Proceedings 10th IEEE international workshop on robot and human interactive communication. Roman 2001 (Cat. no. 01th8591). IEEE, 2001.
17. Zhang, Yanjun, Gang Tao, and Mou Chen. "Relative degrees and adaptive feedback linearization control of T–S fuzzy systems." IEEE Transactions on Fuzzy systems 23.6 (2015): 2215-2230.
18. Mian, Ashfaq Ahmad, and Wang Daobo. "Modeling and backstepping-based nonlinear control strategy for a 6 DOF quadrotor helicopter." Chinese Journal of Aeronautics 21.3 (2008): 261-268.
19. Abro, Ghulam E. Mustafa, et al. "Fuzzy Based Backstepping Control Design for Stabilizing an Underactuated Quadrotor Craft under Unmodelled Dynamic Factors." Electronics 11.7 (2022): 999.
20. Wei, Yuhao, Li Sun, and Zhongxian Chen. "An improved sliding mode control method to increase the speed stability of permanent magnet synchronous motors." Energies 15.17 (2022): 6313.
21. Hodgkin, Alan L., and Andrew F. Huxley. "A quantitative description of membrane current and its application to conduction and excitation in nerve." The Journal of physiology 117.4 (1952): 500.
22. Yang, Simon X., and Max Meng. "An efficient neural network approach to dynamic robot motion planning." Neural networks 13.2 (2000): 143-148.
23. Zhu, Daqi, and Bing Sun. "The bio-inspired model based hybrid sliding-mode tracking control for unmanned underwater vehicles." Engineering Applications of Artificial Intelligence 26.10 (2013): 2260-2269.

 doi:10.20944/preprints202408.2173.v1

24. Mu, Bingxian, Yuanyang Pei, and Yang Shi. "Integral sliding mode control for a quadrotor in the presence of model uncertainties and external disturbances." 2017 American control conference (ACC). IEEE, 2017.
25. Xiong, Jing-Jing, and En-Hui Zheng. "Position and attitude tracking control for a quadrotor UAV." ISA transactions 53.3 (2014): 725-731.
26. Xu, Zhe, et al. "A hybrid tracking control strategy for an unmanned underwater vehicle aided with bioinspired neural dynamics." IET Cyber-Systems and Robotics 4.3 (2022): 153-162.
27. Almakhles, Dhafer J. "Robust backstepping sliding mode control for a quadrotor trajectory tracking application." IEEE Access 8 (2019): 5515-5525.
28. Zhao, Wanbing, Hao Liu, and Xinlong Wang. "Robust visual servoing control for quadrotors landing on a moving target." Journal of the Franklin Institute 358.4 (2021): 2301-2319.
29. Zhang, Xu, et al. "Autonomous flight control of a nano quadrotor helicopter in a GPS-denied environment using on-board vision." IEEE Transactions on Industrial Electronics 62.10 (2015): 6392-6403.
30. Grossberg, Stephen. "Nonlinear neural networks: Principles, mechanisms, and architectures." Neural networks 1.1 (1988): 17-61.
31. Abro, Ghulam E. Mustafa, et al. "Review of hybrid control designs for underactuated quadrotor with unmodelled dynamic factors." Emerging Technologies in Computing: Third EAI International Conference, iCETiC 2020, London, UK, August 19–20, 2020, Proceedings 3. Springer International Publishing, 2020.
32. Wang, Ning, et al. "Hybrid finite-time trajectory tracking control of a quadrotor." ISA transactions 90 (2019): 278-286.
33. Maaruf, Muhammad, Waleed M. Hamanah, and Mohammad A. Abido. "Hybrid Backstepping Control of a Quadrotor Using a Radial Basis Function Neural Network." Mathematics 11.4 (2023): 991.
34. Raffo, Guilherme V., Manuel G. Ortega, and Francisco R. Rubio. "Robust nonlinear control for path tracking of a quad-rotor helicopter." Asian Journal of Control 17.1 (2015): 142-156.
35. Jia, Zhenyue, et al. "Integral backstepping sliding mode control for quadrotor helicopter under external uncertain disturbances." Aerospace Science and Technology 68 (2017): 299-307.